https://doi.org/10.5194/egusphere-2025-6571
Preprint. Discussion started: 6 February 2026

Atmospheric gravity waves observed in Brazil on 14 October 2023

Anderson Vestena Bilibio [1], Igo Paulino [1], Cristiano Max Wrasse [2], Prosper Kwamla Nyassor [2], Ricardo Arlen Buriti [1], Cosme Alexandre de Oliveira Barros Figueiredo [1], Fábio Egito [1], Hisao Takahashi [2], Toyese Tunde Ayorinde [2], Lucas Vaz Peres [3], and Rodrigo da Silva [3]

[1]Unidade Acadêmica de Física, Universidade Federal de Campina Grande, Campina Grande/PB, Brazil.
[2]Divisão de Clima Espacial, Instituto Nacional de Pesquisas Espaciais, São José dos Campos/SP, Brazil.
[3]Departamento de Física, Universidade Federal do Oste do Pará, Santarém/PA, Brazil.

Correspondence: Anderson Vestena Bilibio (andersonvestenabilibio05@gmail.com)

Abstract.

This study investigates the characteristics and origins of atmospheric gravity waves (AGWs) observed over Brazil following the annular solar eclipse of 14 October 2023. Utilizing a network of all-sky imagers located at Santarém, São João do Cariri and Bom Jesus da Lapa. Some medium- and small-scale gravity waves were identified in the mesosphere and lower thermosphere (MLT) via airglow emissions. To determine the likely sources of these waves, a reverse ray-tracing method was employed, incorporating empirical wind (HWM14) and temperature (NRLMSISE-00) models, alongside top cloud temperature data to account for tropospheric convection. Analysis of four distinct wave cases revealed a complex spectrum of propagation dynamics. At São João do Cariri, both a medium-scale wave (horizontal wavelength, $\lambda_H = 174.4$ km) and a small-scale wave ($\lambda_H = 21.3$ km) were traced back to stratospheric altitudes where their trajectories intersected the Moon's shadow. The absence of local convective systems suggests these waves were likely triggered by eclipse-induced atmospheric cooling. At Santarém, a large-scale wave ($\lambda_H = 1523.8$ km) with a high phase speed (218 m/s) was found to originate near the eclipse path at the tropopause. Conversely, a wave observed at Bom Jesus da Lapa ($\lambda_H = 635.5$ km), while geographically near the eclipse path, showed temporal and spatial alignment with tropospheric convection rather than the elipse path. These findings highlight the dual role of solar eclipses and convective processes in generating AGWs and demonstrate the efficacy of ray-tracing in distinguishing between transient astronomical triggers and persistent meteorological sources.

1 Introduction

Atmospheric gravity waves are generated by oscillatory phenomena within Earth's atmosphere. They are essential for understanding whole-atmosphere dynamics and the coupling between the lower and upper atmosphere. Additionally, gravity waves play a crucial role in transferring energy and momentum through these layers, contributing to the overall energy balance (Fritts and Alexander, 2003).

Due to the complexity of the generation processes of the gravity waves and their impact on the energy budget, identifying likely sources remains a current and vital focus in atmospheric science. While gravity waves are most commonly generated by convection (Vadas et al., 2009), wind shear (Clemesha and Batista, 2008), and orography (Liu et al., 2024), transient events

https://doi.org/10.5194/egusphere-2025-6571
Preprint. Discussion started: 6 February 2026

such as solar eclipses can also produce them (Paulino et al., 2020). Understanding the characteristics of these waves is essential for evaluating their actual impact on the atmosphere.

The generation of gravity waves by a solar eclipse was first proposed by Chimonas and Hines (1970). They suggested that the localized and rapid cooling of the atmosphere in the wake of the moon's umbra creates a pressure perturbation similar to a bow wave. This process can trigger atmospheric gravity waves that propagate into the upper atmosphere, generating traveling ionospheric disturbances (TIDs) moving at supersonic speeds. Observations during the total solar eclipse on March 7, 1970, provided evidence for such waves, which manifested as TIDs propagating at speeds of approximately 600-800 m/s (Lerfald et al., 1972).

After that, many observations have reveled relevant characteristics of gravity waves generated by the solar eclipse as in the neutral atmosphere as in the ionosphere. Several publications have pointed out characteristics of gravity waves in different part of the world and under different obscuration, a quick revision of these works can be found in (Paulino et al., 2020).

Solar eclipses are typically diurnal events that occur during the New Moon phase. Consequently, all observed gravity waves generated by eclipses occur during the daytime and observations are typically conducted throughout the day of the eclipse. The total solar eclipse of 21 August 2017 possessed unique characteristics, as it concluded over the middle of the South Atlantic Ocean. Due to its proximity to the Brazilian coast, an experiment was conducted that allowed for the observation of bow waves in the thermosphere Harding et al. (2018) and gravity waves (Paulino et al., 2020) in the mesopause. These observations utilized nighttime airglow over São João do Cariri (7.4^{o}S. 36.5^{o}W). In the latter case, a long gravity wave with a horizontal wavelength of 1,620 km and a period of 2.5 hours propagated from the Atlantic toward the land over a distance of two thousand kilometers.

Subsequently, an observational campaign was conducted in Chile to investigate the atmospheric response to the 2 July 2019 total solar eclipse. The authors also observed gravity waves using airglow imaging. However, in that instance, the spectral parameters were distinct, characterized by short periods and wavelengths (Vargas et al., 2022). In addition to the airglow observations, other instruments were utilized that contributed significantly to understanding the impact of bow waves generated by the eclipse in the mesosphere and lower thermosphere (MLT).

The annular solar eclipse of 14 October 2023 featured a unique scenario to investigate atmospheric gravity waves over Brazil. First, the path of the eclipse concluded very near the coast, ie., the Moon's shadow (specifically the umbra) crossed the region monitored by the São João do Cariri observatory before moving over the ocean. Second, because it was an annular eclipse, the 'ring of fire' manifestation meant the atmosphere remained partially illuminated throughout the event. Furthermore, two additional stations were operational during the event: Santarém (2.4^{o}S. 54.7^{o}W) and Bom Jesus da Lapa (13.2^{o}S. 43.4^{o}W), located to the north and south of São João do Cariri, respectively.

This work presents the characteristics of gravity waves observed across the three stations, including their atmospheric trajectories calculated using the ray tracing method. Furthermore, salient results regarding the likely sources of these waves, specifically the potentially generated by the eclipse, are presented and discussed.

https://doi.org/10.5194/egusphere-2025-6571
Preprint. Discussion started: 6 February 2026

2 Observations and methodology

In this work, three all-sky imagers were used to characterize gravity waves observed on 14 October 2023. These instruments were deployed in Santarém, São João do Cariri, and Bom Jesus da Lapa. These facilities are part of the Brazilian Study and Monitoring of Space Weather (EMBRACE, acronym for the Portuguese version) program, which was established for space weather monitoring. The Brazilian space weather program maintains a broader network of instruments spread throughout the country.

The all-sky imagers were manufactured by Keo Scientific Inc. Each unit features a fish-eye lens (f/4), a 3-inch interference filter wheel, a telecentric lens system and a charge-coupled device (CCD) chip. Further technical specifications regarding the imagers used in this study are available in Wrasse et al. (2024). This instrumentation has been used to investigate small- and medium-scale gravity waves (Essien et al., 2018), periodic waves in the thermosphere (Paulino et al., 2016) and single-front traveling ionospheric disturbances (TIDs), as well as other ionospheric irregularities (Wrasse et al., 2021). The filter wheel allows for the inclusion of various interference filters used to monitor different atmospheric regions. Specifically, emissions of OH (peaking at 87 km) and OI 5577 (peaking at 96 km) were used to observe the mesosphere and lower thermosphere (MLT), while OI 6300 emission (peaking at 250 km) was used to monitor the thermosphere.

Figure 1 shows the path of the Moon's shadow across South America, ending in the Atlantic Ocean. The locations of Santarém, São João do Cariri, and Bom Jesus da Lapa are marked on the map, along with the approximate fields of view (FOV) for the all-sky images of MLT emissions (indicated by dotted circles). The timing of the Moon's shadow (in UTC) is displayed in the white boxes. Although the path of the shadow crosses the FOV of the imagers, it is important to note that airglow observations began only after local sunset, as the equipment is highly sensitive to background light.

To calculate gravity wave parameters (horizontal wavelength, period and propagation direction), two distinct techniques were employed: (i) two-dimensional Fourier analysis using cross-spectra (Garcia et al., 1997; Wrasse et al., 2006) and (ii) keogram analysis (Shiokawa et al., 2009; Paulino et al., 2011). The former provides greater precision for small-scale waves, whereas the latter is applicable to both scales but is particularly effective for investigating medium-scale waves.

In order to calculate the retro trajectory of gravity waves in the atmosphere, the ray-tracing method was used. It consists of regressing the wave propagation from the observation point back to the Earth's surface. The methodology follows the approach described by Vadas (2007), which involves simultaneously solving the set of equations for position and wavevector in a medium where background changes are governed by wind and temperature variations. The equation can be written as:

$$\frac{dx_i}{dt} = V_i + \frac{\partial \omega_{Ir}}{\partial k_i} = V_i + c_{g_i} \tag{1}$$

and

$$\frac{dk_i}{dt} = -k_j \frac{\partial V_j}{\partial x_i} - \frac{\partial \omega_{Ir}}{\partial x_i} \ , \tag{2}$$

https://doi.org/10.5194/egusphere-2025-6571
Preprint. Discussion started: 6 February 2026

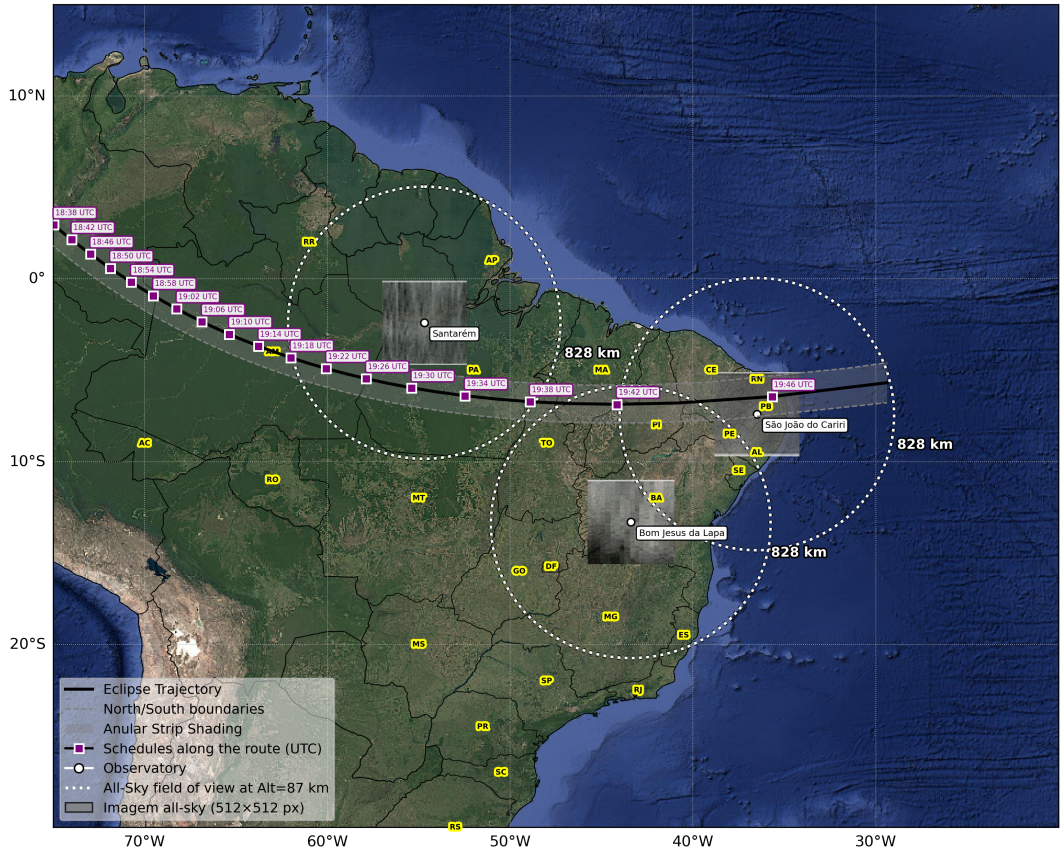

Figure 1. Illustration of the solar eclipse trajectory over Brazil (black line), including the north and south boundaries of the annular strip (gray dashed line) and the corresponding times along the path in UTC marked by purple squares. Brazilian states are shown in the figure using abbreviations in yellow boxes. The locations of the airglow observation sites are marked by white dots. For each site, identified atmospheric gravity wave patterns are shown, derived from processed all-sky airglow images with projection of 512 km x 512 km. The field of viwe of the imagers projecte on the Earth surface are indicated by the dotted circles considering a altitude of observation around 87 km. It is important to note that all maps in this work were generated using Cartopy (Met Office, 2010–2025).

where x_i represents the position of the wave packet, V_i is the background wind vector, ω_{Ir} is the intrinsic frequency of the wave, k_i is the wave vector and c_{g_i} is the group velocity vector of the wave.

In addition to gravity wave parameters, the model requires background temperature and wind data for each interaction. The present work utilizes empirical models to provide these inputs. The Horizontal Wind Model (HWM-14) (Drob et al., 2008, 2015) provided vertical profiles for meridional and zonal wind components with a vertical resolution of 2 km and a temporal cadence of 2 hours. Using the same resolutions, the Naval Research Laboratory Mass Spectrometer and Incoherent Scatter model (NRLMSISE-00) (Picone et al., 2002) was used to generate the temperature profiles. This ray-tracing method-

https://doi.org/10.5194/egusphere-2025-6571
Preprint. Discussion started: 6 February 2026

ology, with these inputs, has been used successfully to investigate likely sources of gravity waves in the equatorial region (Sivakandan et al., 2016).

Supplementary information used in this work includes the eclipse trajectory (Espenak, 2023) and cloud-top temperature (INPE, 2024). These data are available online.

3 Results and discussion

Several atmospheric gravity waves were observed over the three Brazilian sites on the night of 14-15 October 2023. Using two-dimensional cross-spectrum and keogram analysis, many of these waves were identified and their horizontal parameters were calculated. Table 1 summarizes the parameters of the four gravity waves selected for reverse ray-tracing. These specific waves were chosen based on their potential to intercept the Moon's shadow across their paths. The observed parameters of these gravity waves align with previous findings (Essien et al., 2018).

Table 1. Summary of gravity wave events observed during the annular solar eclipse of 14 October 2023 at the three sites in Brazil.

Nr	Observation Site	Emis.	λ_H (km)	τ (min)	c_H (m/s)	Dir.
001	São João do Cariri-PB	OH	174.43	58.62	49.60	SE
002	São João do Cariri-PB	OI5577	21.30	22.80	15.60	SE
003	Santarém-PA	OH	1523.82	116.51	217.98	West
004	Bom Jesus da Lapa-BA	OH	635.45	69.50	152.38	SE

Figure 2 shows the projection of the ray path for a gravity wave observed at São João do Cariri over a map. The parameters of this gravity wave are shown on the legend box. The solid cyan line represents the reverse trajectory using a wind model as input, while the dashed red lines indicate the trajectory if no wind is considered in the ray-tracing calculations. Cloud top temperatures are indicated at specific locations and referenced in the colorbar. The point where the ray path touches the ground is represented by a red star. The solid black line represents the path of the eclipse and the filled black circle represents the point where the gravity wave ray path intercepts the eclipse path. These same elements are reproduced in the figures shown below for other case studies as well.

https://doi.org/10.5194/egusphere-2025-6571
Preprint. Discussion started: 6 February 2026

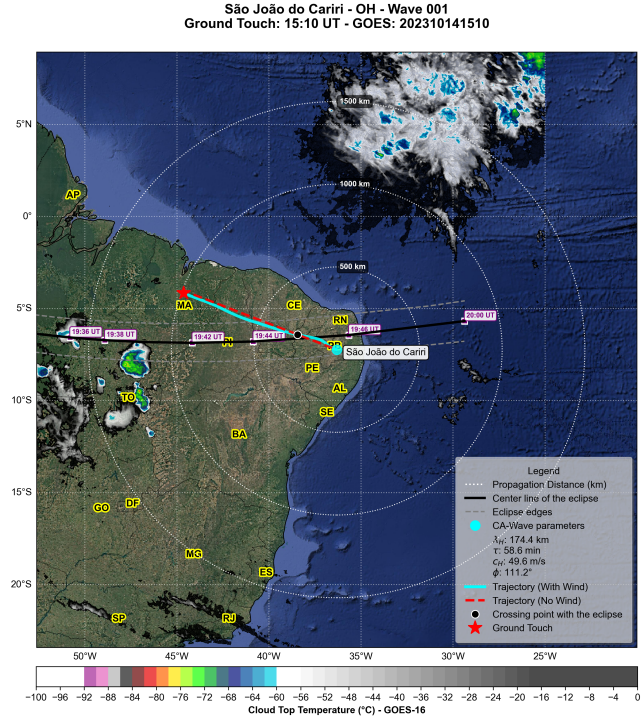

Figure 2. Horizontal backward trajectories for the gravity wave 001, calculated using ray tracing both with wind (solid cyan line) and without wind (dashed red line), are shown on the map. São João do Cariri is represented by a filled cyan circle, while the red star indicates the location where the gravity wave reached the ground. The eclipse path is included, following the same conventions described in Figure 1. Concentric white circles represent iso-distances at 500 km, 1000 km, and 1500 km from the observatory. The black circle marks the point where the ray path and the eclipse path intersect. Cloud top temperatures, derived from the GOES-16 satellite at 15:10 UTC, are displayed as colored regions corresponding to the colorbar. Finally, the gravity wave parameters are provided in the legend box.

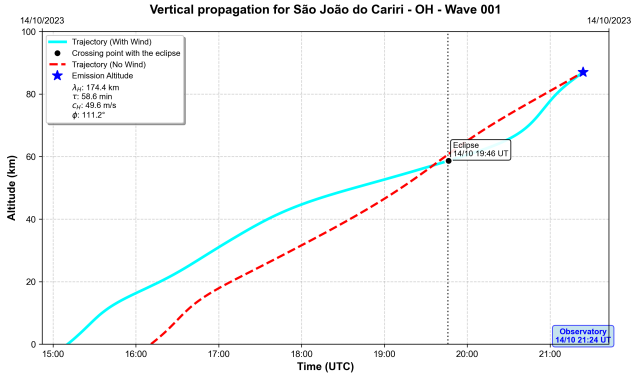

Figure 3. Temporal evolution of the vertical trajectory for gravity wave 001 calculated via ray tracing. The solid cyan line represents the trajectory using the wind model, while the red dashed line represents the no-wind case. The vertical dotted line indicates the time in which the horizontal ray path crossed the eclipse path and the black circle shows the point of intersection between the ray path and the eclipse path. Gravity wave 001 parameters are provided in the legend.

The gravity wave 001 analyzed in Figure 2 had a horizontal wavelength of 174.4 km, a period of 58.6 min and a phase speed of 49.6 m/s, propagating at an azimuth of 111.6° from the north. This indicates a medium-scale gravity wave propagating toward the southeast, suggesting a generation source to the northwest. Following the reverse ray path for this wave, no convective sources were observed in the region northwest of the observatory. Conversely, the trajectory of this wave intersected the path of the eclipse near the observatory.

https://doi.org/10.5194/egusphere-2025-6571
Preprint. Discussion started: 6 February 2026

Figure 3 illustrates the vertical evolution as a function of time to assess the temporal compatibility of the ray path. The symbology remains consistent with Figure 2. Specifically, the vertical dashed line represents the exact time at which the horizontal lines from Figure 2 intersect the eclipse path. The resulting intercept altitude is approximately 55 km (stratospheric altitude).

The Earth's stratosphere is highly sensitive to changes in the temperature profiles during the passage of solar eclipses. For instance, evidence shows cooling of up to 10 K at altitudes of approximately 55–60 km during 26 February 1979 solar eclipse (Schmidlin and Olsen, 1984). Such perturbations in the temperature profile have the potential to generate instabilities, which can, in turn, trigger gravity waves. (Paulino et al., 2020) suggested that the gravity waves observed on 21 August 2017 over São João do Cariri following a total solar eclipse also originated in the stratosphere. Furthermore, the absence of convection in the troposphere near the ray path crossing supports the conclusion that the eclipse was indeed the source of these waves.

Figure 4 and Figure 5 illustrate the ray paths for a gravity wave 002 with a wavelength of 21.3 km and a period of 22.8 min, propagating southeastward (135^o from the North). These figures are analogous to Figure 2 and Figure 3, respectively. Once again, no convective systems were observed in the region where the ray path touchs the ground, suggesting that convection was not the likely source of this wave. However, for both wind and no-wind calculations, the ray paths intersect the eclipse path at stratospheric altitudes. This indicates that changes in the vertical structure of the atmosphere induced by the eclipse may be the probable source.

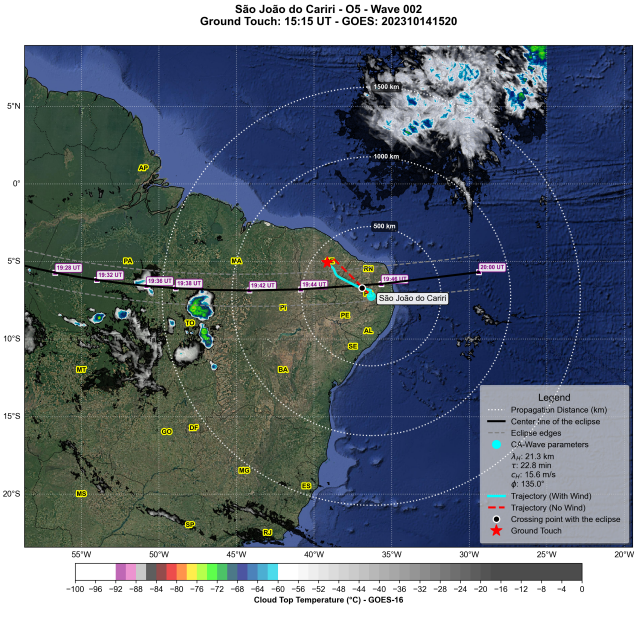

Figure 4. Horizontal backward trajectories for gravity wave 002, observed at São João do Cariri in the OI 5577 emission on 14 October 2023. The elements of this figure are the same as in Figure 2.

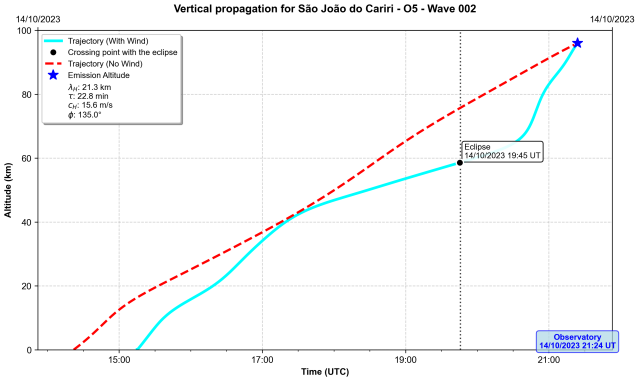

Figure 5. Temporal evolution of the vertical trajectory for gravity wave 002 using the same elements described in Figure 3.

https://doi.org/10.5194/egusphere-2025-6571
Preprint. Discussion started: 6 February 2026

Unlike the first case discussed above and the report by Paulino et al. (2020), which involved medium-scale gravity waves, the present case is classified as a small-scale wave due to its horizontal wavelength. During the total solar eclipse of 2 July 2019, Vargas et al. (2022) identified a gravity wave with a horizontal wavelength of ∼150 km. While this is of the same order as the first wave discussed in this paper, it is significantly longer than the wavelength observed in the present case. Even the phase speed of this wave being relatively slow, the proximity of the observatory to the path of the Moon's shadow allowed for the observation of this wave type in the airglow images. Although the ray-tracing calculations using model winds produced a slight discrepancy in the wave trajectory compared to the no-wind scenario, the final ground position and the temporal evolution of the vertical path showed significant similarities. This indicates that potential errors resulting from the absence of direct wind measurements are not highly significant for this approach.

Figure 6 and Figure 7 show the ray path for a gravity wave 003 observed very late at Santarém. This wave had a horizontal wavelength of 1523.8 km and an observed period of 116.5 min, resulting in a fast phase speed of 218 m/s propagating north-westward with an azimuth of 286.5^o from the North. This particular wave has a high potential to propagate over long distances into the atmosphere without being filtered by the wind, note that there is practically no difference between the trajectories with and without wind. These parameters are compatible with the nighttime waves observed in Brazil after the total solar eclipse of 21 August 2017 (Harding et al., 2018; Paulino et al., 2020).

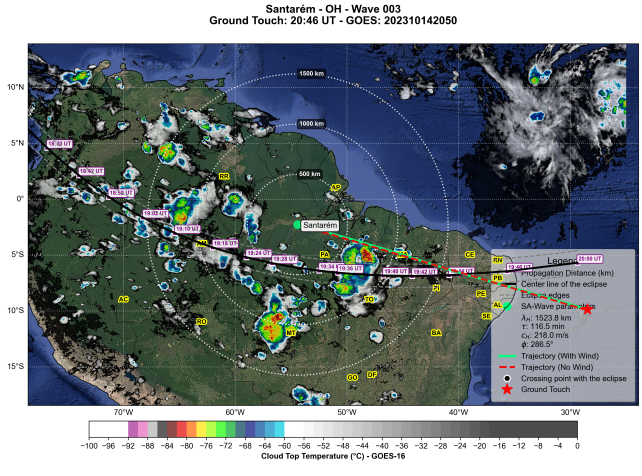

Figure 6. Horizontal backward trajectories for gravity wave 003, observed at São João do Cariri in the OI 5577 emission on 14 October 2023. The elements of this figure are the same as in Figure 2.

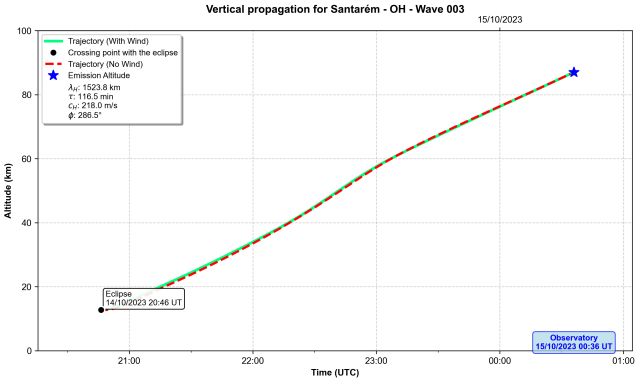

Figure 7. Temporal evolution of the vertical trajectory for gravity wave 003 using the same elements described in Figure 3.

The first thing that call the attention is that the propagation direction is almost in opposition of the two cases observed at São João do Cariri. Looking the ray path for the gravity wave over the map, which has the top cloud temperature overplotted to the time close the wave is getting the troposphere range, one can observe several convective system with potential to generate gravity waves (Vadas et al., 2009). Several hotspots of very high cloud in the Amazon region were presented at that time, however, around the final reverse position of the ray path, there is no potential convective source around.

https://doi.org/10.5194/egusphere-2025-6571
Preprint. Discussion started: 6 February 2026

Observing the temporal evolution of the vertical trajectory in Figure 7, the gravity wave crossed the stratosphere during the nighttime without direct influence from the solar eclipse. However, the ray path intersects the eclipse path in the troppause at approximately 20:50 UTC. Previous works have reported cooling in the tropopause during solar eclipses (Das et al., 2023; Basha et al., 2025). Although the magnitude of this cooling is only a few Kelvins, it disturbs the vertical temperature structure, creating instabilities with the potential to generate waves. The supersonic motion of the lunar shadow remains the most likely mechanism responsible for generating this gravity wave.

To illustrate the complexity of the gravity wave spectrum observed in airglow images, consider an interesting case study from Bom Jesus da Lapa. This particular gravity wave 004 featured a horizontal wavelength of 635.5 km and a period of 69.5 min, propagating toward the southeast (110.1^o). Classified as a medium-scale wave with a high horizontal phase speed of 152.4 m/s, its spectral characteristics suggest it is less susceptible to atmospheric filtering. Consequently, such waves are capable of propagating over long distances and have the potential to penetrate into high altitudes, reaching the thermosphere-ionosphere altitudes (Vadas and Fritts, 2005; Paulino et al., 2012).

Figure 8 and Figure 9 illustrate the ray paths for the gravity wave observed at Bom Jesus da Lapa. In practice, there are no significant differences between the ray paths with and without wind input, which confirms the high propagation capability of this wave through the atmosphere.

Due to the fast phase speed, the reverse ray path of the gravity wave reaches the surface at 00:52 UTC (Figure 9), which is significantly later than the passage of the Moon's shadow near that region. Therefore, it is unlikely that this wave was excited by the eclipse. On the other hand, several convective processes were active near the position where the ray path crosses the troposphere/tropopause. This suggests that the wave was likely generated by convection, as the influence of a convective cell can extend for hundreds of kilometers (Vadas et al., 2009).

https://doi.org/10.5194/egusphere-2025-6571
Preprint. Discussion started: 6 February 2026

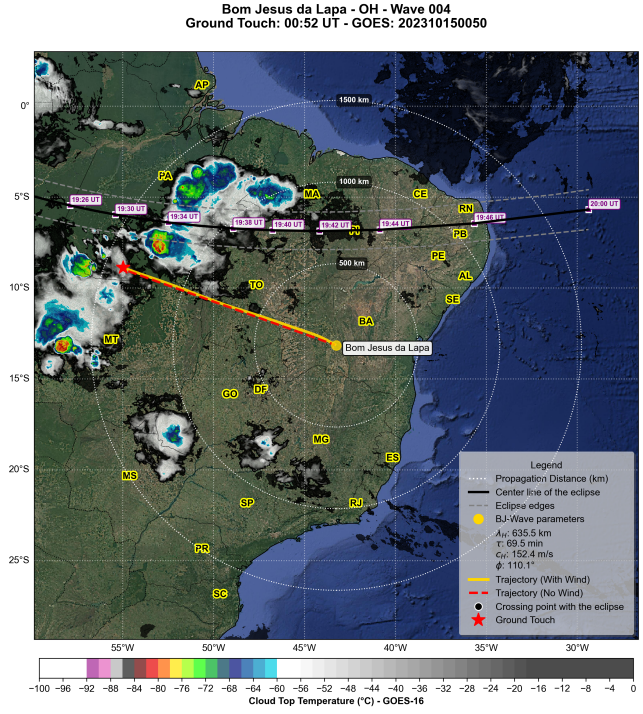

Figure 8. Horizontal backward trajectories for gravity wave 004, observed at São João do Cariri in the OI 5577 emission on 14 October 2023. The elements of this figure are the same as in Figure 2.

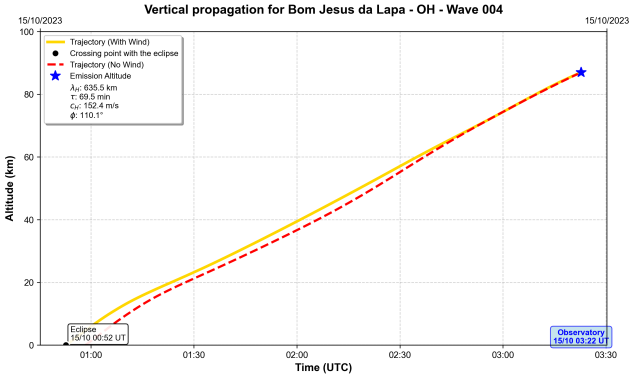

Figure 9. Temporal evolution of the vertical trajectory for gravity wave 004 using the same elements described in Figure 3.

Although this gravity wave exhibits characteristics similar to other case studies presented here and in previous works, the ray-tracing results suggest that it is unlikely to have been excited by the eclipse. This evidence highlights the complexity of the gravity wave spectrum observed in airglow images, which can originate from various sources.

Several other small- and medium-scale gravity waves were observed in all three sites (not shown here). However, only structures with propagation directions potentially linked to the eclipse were considered. Furthermore, the difficulty of isolating quasi-monochromatic waves within the complex image spectrum limits the number of waves available for ray-tracing calculations.

4 Conclusions

Airglow observations conducted on the night of 14-15 October 2023, following the annular solar eclipse, at Santarém, São João do Cariri and Bom Jesus da Lapa revealed a complex spectrum of small- and medium-scale gravity waves. Among these, four specific cases were selected to investigate their atmospheric propagation using reverse trajectories calculated via a ray-tracing method. The primary objective was to identify the likely sources of these gravity waves. To achieve this, the temporal evolution

https://doi.org/10.5194/egusphere-2025-6571
Preprint. Discussion started: 6 February 2026

of the Moon's shadow and top cloud temperatures were synchronized with the moments the ray paths reached the ground. The main findings are summarized as follows:

- Observed at São João do Cariri, a medium-scale gravity wave (horizontal wavelength of 174.4 km and period of 58.6 min) featured a ray path intersecting the Moon's shadow at stratospheric altitudes. Given the absence of tropospheric convective systems at the time of ground-level arrival, the eclipse is identified as the likely source of excitation;

- A small-scale gravity wave (wavelength of 21.3 km and period of 22.8 min) observed at São João do Cariri exhibited vertical and horizontal propagation characteristics that allowed it to avoid filtering by either turning or critical levels. Because the ray path intercepted the Moon's shadow in the stratosphere and no convective systems were present in the troposphere to serve as a source, the eclipse is a strong candidate for exciting of this wave as well;

- Reverse ray-tracing analysis suggests that a very large gravity wave (horizontal wavelength of 1523.8 km and period of 116.5 min) observed at Santarém could propagate over a long distance until reaching the eclipse path in the tropopause. Although the horizontal path crossed several convective systems in the central region of Brazil, by the time it reached the tropopause, only the Moon's shadow had the potential to excite the gravity waves;

- The final case study observed at Bom Jesus da Lapa indicates that a gravity wave (wavelength of 635.5 km and a period of 69.5 min) could have propagated over a long distance, placing its tropospheric origin near the eclipse path. However, the vertical propagation time was relatively short and did not coincide with the passage of the eclipse. Furthermore, certain convective systems in the troposphere show high potential for generating this specific wave.

These results corroborate the ray-tracing method as a highly effective tool for studying gravity wave propagation through the atmosphere, particularly when gravity wave phase speeds are high. This approach is especially valuable for identifying gravity wave sources, as it provides both the tropospheric point of origin and the temporal evolution of vertical propagation. Furthermore, incorporating tropospheric meteorological parameters, such as cloud-top temperature, significantly enhances the potential of the method.

Data availability. Airglow images are available on line at https://www2.inpe.br/climaespacial/. Top cloud temperature can be downloaded at https://data.inpe.br/.

Code and data availability. It can be requested to the corresponding author.

Author contributions. AVB - writing and data analysis; IP - writing, scientific conception and experiment; The other authors - Experiment and revision.

https://doi.org/10.5194/egusphere-2025-6571
Preprint. Discussion started: 6 February 2026

Competing interests. Igo Paulino is a member of the editorial board of Annales Geophysicae.

Acknowledgements. This work has been financed by the Fundação de Amparo à Pesquisa do Estado da Paraíba (72736.1300.35596.03012025) and by the Conselho Nacional de Desenvolvimento Científico e Tecnológico (CNPQ, grant number 309981/2023-9).

https://doi.org/10.5194/egusphere-2025-6571
Preprint. Discussion started: 6 February 2026

References

Basha, G., Ratnam, M. V., Jiang, J. H., and Pangaluru, K.: Investigating the Effects of the Solar Eclipse on the Atmosphere over Land and Oceanic Regions: Observations from Ground Stations and COSMIC2 Data, Atmosphere, 16, 872, https://doi.org/10.3390/atmos16070872, 2025.

Chimonas, G. and Hines, C.: Atmospheric gravity waves induced by a solar eclipse, Journal of Geophysical Research, 75, 875–875, 1970.

Clemesha, B. and Batista, P.: Gravity waves and wind-shear in the MLT at 23^{o}S, Advances in Space Research, 41, 1472–1477, https://doi.org/https://doi.org/10.1016/j.asr.2007.03.085, 2008.

Das, S. S., Kishore Kumar, K., Subrahmanyam, K. V., Venkat Ratnam, M., Suneeth, K. V., Sunilkumar, S. V., Sinha, P. R., Ghosh, A. K., Das, S. K., Sonwabne, S., Muralikrishna, U. V., Kolte, Y., Naja, M., Abhilash, S., Satheesan, K., Rakesh, V., Mahesh, P., Koushik, N., Satheesh Chandran, P. R., Girach, I. A., Namboodiri, K. V. S., Pandithurai, G., and Kirankumar, N. V. P.: Impact of Annular Solar Eclipse on the Trace Gases and Dynamics of the Lower and Middle Atmosphere: Results Inferred From an Integrated Campaign "Suryagrahan-2019", Earth and Space Science, 10, e2023EA003 044, https://doi.org/10.1029/2023EA003044, 2023.

Drob, D., Emmert, J., Crowley, G., Picone, J., Shepherd, G., Skinner, W., Hays, P., Niciejewski, R., Larsen, M., She, C., et al.: An empirical model of the Earth's horizontal wind fields: HWM07, Journal of Geophysical Research: Space Physics, 113, 2008.

Drob, D. P., Emmert, J. T., Meriwether, J. W., Makela, J. J., Doornbos, E., Conde, M., Hernandez, G., Noto, J., Zawdie, K. A., McDonald, S. E., et al.: An update to the Horizontal Wind Model (HWM): The quiet time thermosphere, Earth and Space Science, 2, 301–319, 2015.

Espenak, F.: Path of Annular Solar Eclipse of 2023 Oct 14, NASA Goddard Space Flight Center, https://eclipse.gsfc.nasa.gov/SEpath/SEpath2001/SE2023Oct14Apath.html, accessed: 2024-12-30, 2023.

Essien, P., Paulino, I., Wrasse, C. M., Campos, J. A. V., Paulino, A. R., Medeiros, A. F., Buriti, R. A., Takahashi, H., Agyei-Yeboah, E., and Lins, A. N.: Seasonal characteristics of small- and medium-scale gravity waves in the mesosphere and lower thermosphere over the Brazilian equatorial region, Annales Geophysicae, 36, 899–914, https://doi.org/10.5194/angeo-36-899-2018, 2018.

Fritts, D. C. and Alexander, M. J.: Gravity wave dynamics and effects in the middle atmosphere, Reviews of Geophysics, 41, 1003, https://doi.org/10.1029/2001RG000106, 2003.

Garcia, F., Taylor, M. J., and Kelley, M.: Two-dimensional spectral analysis of mesospheric airglow image data, Applied optics, 36, 7374–7385, 1997.

Harding, B. J., Drob, D. P., Buriti, R. A., and Makela, J. J.: Nightside Detection of a Large-Scale Thermospheric Wave Generated by a Solar Eclipse, Geophysical Research Letters, 45, 3366–3373, https://doi.org/10.1002/2018GL077015, 2018.

INPE: Cloud Top Temperature - INPE Geospatial Data Portal, https://data.inpe.br/, 2024.

Lerfald, G., Jurgens, R., Vesecky, J., and Washburn, T.: Traveling ionospheric disturbances observed near the time of the solar eclipse of 7 March 1970, Journal of Atmospheric and Terrestrial Physics, Volume 34, Issue 4, Pages 733–741, https://doi.org/https://doi.org/10.1016/0021-9169(72)90161-4, 1972.

Liu, Y., Chen, Z., Fan, Z., Zhou, C., Wang, X., Zhang, Y., Zhou, Y., Lan, T., and Qing, H.: Statistical analysis on orographic atmospheric gravity wave and sporadic E layer, Journal of Atmospheric and Solar-Terrestrial Physics, 259, 106 256, https://doi.org/https://doi.org/10.1016/j.jastp.2024.106256, 2024.

Met Office: Cartopy: a cartographic python library with a matplotlib interface, Exeter, Devon, https://scitools.org.uk/cartopy, 2010–2025.

Paulino, I., Takahashi, H., Medeiros, A., Wrasse, C., Buriti, R., Sobral, J., and Gobbi, D.: Mesospheric gravity waves and ionospheric plasma bubbles observed during the COPEX campaign, Journal of Atmospheric and Solar-Terrestrial Physics, 73, 1575–1580,

https://doi.org/10.5194/egusphere-2025-6571
Preprint. Discussion started: 6 February 2026

https://doi.org/https://doi.org/10.1016/j.jastp.2010.12.004, influence of Solar Activity on Interplanetary and Geophysical Phenomena, 2011.

Paulino, I., Takahashi, H., Vadas, S. L., Wrasse, C. M., Sobral, J. H. A., Medeiros, A. F., Buriti, R. A., and Gobbi, D.: Forward ray-tracing for medium-scale gravity waves observed during the COPEX campaign, Journal of Atmospheric and Solar-Terrestrial Physics, 90, 117–123, https://doi.org/10.1016/j.jastp.2012.03.009, 2012.

Paulino, I., Medeiros, A. F., Vadas, S. L., Wrasse, C. M., Takahashi, H., Buriti, R. A., Leite, D., Filgueira, S., Bageston, J. V., Sobral, J. H. A., and Gobbi, D.: Periodic waves in the lower thermosphere observed by OI630 nm airglow images, Annales Geophysicae, 34, 293–301, https://doi.org/10.5194/angeo-34-293-2016, 2016.

Paulino, I., Figueiredo, C. A. O. B., Rodrigues, F. S., Buriti, R. A., Wrasse, C. M., Paulino, A. R., Barros, D., Takahashi, H., Batista, I. S., Medeiros, A. F., Batista, P. P., Abdu, M. A., de Paula, E. R., Denardini, C. M., Lima, L. M., Cueva, R. Y., and Makela, J. J.: Atmospheric Gravity Waves Observed in the Nightglow Following the 21 August 2017 Total Solar Eclipse, Geophysical Research Letters, 47, e2020GL088 924, https://doi.org/https://doi.org/10.1029/2020GL088924, 2020.

Picone, J., Hedin, A., Drob, D. P., and Aikin, A.: NRLMSISE-00 empirical model of the atmosphere: Statistical comparisons and scientific issues, Journal of Geophysical Research: Space Physics, 107, SIA–15, 2002.

Schmidlin, F. and Olsen, R.: Modification of the strato-mesospheric temperature and wind structure resulting from the 26 February 1979 solar eclipse, Journal of Atmospheric and Terrestrial Physics, 46, 273–280, https://doi.org/https://doi.org/10.1016/0021-9169(84)90154-5, 1984.

Shiokawa, K., Otsuka, Y., and Ogawa, T.: Propagation characteristics of nighttime mesospheric and thermospheric waves observed by optical mesosphere thermosphere imagers at middle and low latitudes, Earth, planets and space, 61, 479–491, 2009.

Sivakandan, M., Paulino, I., Taori, A., and Niranjan, K.: Mesospheric gravity wave characteristics and identification of their sources around spring equinox over Indian low latitudes, Atmospheric Measurement Techniques, 9, 93–102, https://doi.org/10.5194/amt-9-93-2016, 2016.

Vadas, S. L.: Horizontal and vertical propagation and dissipation of gravity waves in the thermosphere from lower atmospheric and thermospheric sources, Journal of Geophysical Research: Space Physics, 112, A06 305, https://doi.org/10.1029/2006JA011845, 2007.

Vadas, S. L. and Fritts, D. C.: Thermospheric responses to gravity waves: Influences of increasing viscosity and thermal diffusivity, Journal of Geophysical Research: Atmospheres, 110, D15 103, https://doi.org/10.1029/2004JD005574, 2005.

Vadas, S. L., Taylor, M. J., Pautet, P.-D., Stamus, P. A., Fritts, D. C., Liu, H.-L., São Sabbas, F. T., Batista, V. T., Rampinelli, V. T., and Takahashi, H.: Convection: the likely source of the medium-scale gravity waves observed in the OH airglow layer near Brasilia, Brazil, during the SpreadFEx campaign, Annales Geophysicae, 27, 231–259, https://doi.org/10.5194/angeo-27-231-2009, 2009.

Vargas, F., Liu, A., Swenson, G., Segura, C., Vega, P., Fuentes, J., Pautet, D., Taylor, M., Zhao, Y., Morton, Y., and Bourne, H.: Mesosphere and Lower Thermosphere Changes Associated With the 2 July 2019 Total Eclipse in South America Over the Andes Lidar Observatory, Cerro Pachon, Chile, Journal of Geophysical Research: Atmospheres, 127, e2021JD035 064, https://doi.org/10.1029/2021JD035064, 2022.

Wrasse, C. M., Batista, I. S., Takahashi, H., de Paula, E. R., Denardini, C. M., Medeiros, A. F., Paulino, I., Figueiredo, C. A. O. B., Rodrigues, F. S., Buriti, R. A., et al.: Observations of mesospheric gravity waves over São João do Cariri (7.4°S, 36.5°W) using all-sky airglow images—Part 2: Seasonal and interannual variability, Annales Geophysicae, 24, 1721–1730, 2006.

Wrasse, C. M., Figueiredo, C. A. O. B., Barros, D., Takahashi, H., Carrasco, A. J., Vital, L. F. R., Resende, L. C. A., Egito, F., de Matos Rosa, G., and Sampaio, A. H. R.: Interaction between Equatorial Plasma Bubbles and a Medium-Scale Traveling Iono-

https://doi.org/10.5194/egusphere-2025-6571
Preprint. Discussion started: 6 February 2026

spheric Disturbance, observed by OI 630 nm airglow imaging at Bom Jesus de Lapa, Brazil, Earth and Planetary Physics, 5, 397–406, https://doi.org/10.26464/epp2021045, 2021.

Wrasse, C. M., Nyassor, P. K., da Silva, L. A., Figueiredo, C. A. O. B., Bageston, J. V., Naccarato, K. P., Barros, D., Takahashi, H., and Gobbi, D.: Studies on the propagation dynamics and source mechanism of quasi-monochromatic gravity waves observed over São Martinho da Serra (29° S, 53° W), Brazil, Atmospheric Chemistry and Physics, 24, 5405–5431, https://doi.org/10.5194/acp-24-5405-2024, 2024.